Available online at www.sciencedirect.com

SCIENCE DIRECT®

ELSEVIER

Nuclear Instruments and Methods in Physics Research B 241 (2005) 454–458

NIM B
Beam Interactions with Materials & Atoms

www.elsevier.com/locate/nimb

High resolution backscattering studies of nanostructured magnetic and semiconducting materials

A. Fonseca [a,*], N. Franco [a], E. Alves [a,b], N.P. Barradas [a,b], J.P. Leitão [c], N.A. Sobolev [c], D.F. Banhart [d], H. Presting [e], V.V. Ulyanov [f], A.I. Nikiforov [f]

[a] *Instituto Tecnológico e Nuclear, Dept. Fisica, Estrada Nac. 10, 2686-953 Sacavém, Portugal*
[b] *Centro de Física Nuclear da Universidade de Lisboa, Av. Prof. Gama Pinto 2, 1649-003 Lisboa, Portugal*
[c] *Departamento de Física da Universidade de Aveiro, 3810-193 Aveiro, Portugal*
[d] *Z. E. Elektronenmikroskopie, Universität Ulm, Albert-Einstein-Allee 11, D-89069 Ulm, Germany*
[e] *Daimler-Chrysler Forschungszentrum, 89081 Ulm, Germany*
[f] *Institute of Semiconductor Physics, 630090 Novosibirsk, Russia*

Abstract

Low dimension structures raises inevitably new technological challenges in materials science. The new structures must fulfill stringent requirements in composition, crystalline quality and interface sharpness among others. We present and discuss the results of Si/Ge quantum structures and FePt/C multilayer structures deposited at different temperatures by ion beam sputtering. Evidence for the presence of FePt nanoparticles embedded in the C matrix and Ge islands in Ge/Si multilayers structures was found. Size and stoichiometry of the nanoparticles and the multilayer periodicity was obtained using Rutherford backscattering at grazing angles of incidence. The strain state of the single crystalline layers was determined by tilt axis channelling.

PACS: 82.80.Yc; 68.55.Nq; 68.65.Ac; 68.65.Hb

Keywords: High resolution Rutherford backscattering; Multilayers; Nanoparticles

---

1. Introduction

During last decades a strong effort has been made to fabricate optical, electronic and magnetic devices based on multilayer structures. With this purpose, many growth modes of quantum

---

[*] Corresponding author. Tel.: +351 219946104; fax: +351 219941525.
E-mail address: afonseca@itn.pt (A. Fonseca).

0168-583X/$ - see front matter © 2005 Elsevier B.V. All rights reserved.
doi:10.1016/j.nimb.2005.07.093

structures have been studied on Si/Ge system [1–3] and magnetic multilayers [4].

A technique to fabricate Ge islands is epitaxial growth, when lattice mismatch between Si and Ge (4%) and the overgrowth layer allows the formation of self-assembled quantum dots (QD) through the Stranski–Krastanow mechanism (SK).The use of a wetting layer before dots formation has been demonstrated to be an important way of coherent growth of uniform and small dots (~10 nm) with a relatively high density (~10^8 to 10^{10}/cm^2) [5]. Recently, many efforts have been made to grow dots with higher density and less than 10 nm, increasing their quantum efficiency. An ultra thin silicon oxide film has been shown, very recently, to be an effective coverage of Si substrates to obtain Ge dots with an extremely high density (10^{12}/cm^2) and a minimum size [6,7]. These Ge dots are not connected to each other by a Ge wetting layer as in SK method. Recently, it was shown that dot growth in epitaxial relationship with silicon substrate, and after few depositions, is composed of pure Ge [6].

On the other hand, high densities of recording media are also pursued and are expected to reach 100 Gbit/in.^{2} within a few years. Such densities require magnetic grain sizes of 10 nm or less, which is close to the superparamagnetic limit of current media. Potential candidates are the ordered phases of FePt or CoPt, which have very large magnetocrystalline anisotropy, essential to guarantee the thermal stability [4,8]. The major problems with these high density systems are the magnetic coupling between the nanoparticles, and their stoichiometry.

In this study, we analyze the Si/Ge and FePt systems using Rutherford backscattering (RBS) at grazing angles of incidence to determine the stoichiometry of the nanoparticles and the multilayer periodicity as well as the interface roughness. The single-layer Si/Ge crystalline structures were also suited to studies in the channelling mode to get information on the strain state of the layers. We compare the results with high resolution transmission electron microscopy (HRTEM) results to study the structure of these multilayered films. The capabilities of ion beam techniques to get information on few layer systems are explored and prove its applicability where other techniques like small-angle X-ray scattering (GISAXS) and transmission electron microscopy (TEM) are inefficient.

2. Experimental details

The first set of samples contained Si/Ge multilayers with 5 and 10 periods grown by molecular beam epitaxy (MBE) on (100) Si substrates at 700 °C. Each layer consisted of a Si spacer with a nominal thickness of 50 nm and 8 monolayers of Ge. Another set of samples was prepared with Ge thicknesses of 0.3, 0.6 and 0.9 nm deposited on top of 0.5, 0.75 or 1 monolayer (ML) of SiO_2. This structures were also grown by MBE on (100) Si substrates, but at 500 °C.

The magnetic C/(FePt/C)$_{\times 20}$ multilayers were prepared by a dual target ion beam sputtering machine with Ar^+ ions, using a pure C target and a composite target with a Pt foil on a Fe disk. The deposition time was kept constant from sample to sample and only the deposition temperature was varied. Samples A, B and C were deposited at 20 °C, 500 °C and 800 °C, respectively.

RBS analysis was performed with a 2.0 MeV He^+ and the backscattered particles detected with a solid state detector placed at 160° in the Cornell geometry with FWHM of 15 keV. The angle of incidence θ, defined as the angle between the beam and the normal to the sample, varied between 78° and 85°. A high precision (~0.01°) computer controlled goniometer was used to place the samples in position and made the channelling measurements. The beam was 0.2 mm wide and 0.6 mm high, which leads to a small beam spot even at grazing angles. The data were analysed with the code NDF [9].

The microstructure of sample A was investigated by a JEOL-3010 high resolution transmission electron microscope in cross-sectional view.

3. Results and discussion

3.1. Ge/Si multilayers

The typical RBS spectra of the 10 period Ge/Si multilayer samples for two tilt angles are shown in

Fig. 1. Since a code which is able to describe the Ge layers, composed of thin Ge layers in most of the places, but with thicker regions corresponding to the quantum dots, is not available, we first did the data analysis assuming laterally homogeneous layers. This leads to the average thickness (areal density) of the layers. Subsequently we analysed the data assuming that there was extensive interdiffusion of the Ge into the Si, leading to a Gaussian profile of Ge concentration. This is a convenient, but inaccurate, method of representing the changing Ge concentration.

As can be seen in Fig. 1, the fitted peaks considering laterally homogeneous layers are better defined than the data, which is due to the fact that the Ge layers are not laterally homogeneous. The extracted structure from the fit indicates a 190 nm thick Si layer at the surface and an average Si layer thickness of 50(3) nm. The average Ge layer thickness is 1.1 (1) nm thick assuming bulk densities. It must be pointed out that while this may be true for the Si, it is not for the Ge. The full width at half maximum of the fitted Ge distribution is 20.5 nm. In this approximation, this value approximately represents the maximum Ge layer thickness. This analysis compares well with the 17.7 nm value determined with TEM shown in Fig. 2. The presence of Ge quantum dots is evident in the TEM picture. It is obvious that our numerical analysis does not allow us to determine the quantum dot density but this information might be obtained using an improved data analysis code.

For the single Ge layer grown over 1 ML of SiO_2 we were able to measure the average thickness and strain. The best fit of the spectra obtained at 78° for the 0.3 and 0.9 nm of Ge (not shown) gives a thickness of 0.28 and 1.2 nm, respectively. The value obtained for the thicker layer is slightly higher than expected even considering an experimental error of ~5%. The strain in the films was evaluated using the channelling curves along the main axial directions. The $\langle 111 \rangle$ and $\langle 110 \rangle$ angular scans were performed along the (110) and (100) planes, respectively. For the 0.3 nm Ge monolayer the angular scans overlap with the Si suggesting a perfect incorporation of the Ge ions in the Si structure. This excludes the formation of Ge quantum dots in agreement with the first photoluminescence studies (to be published) of this sample. The angular curves obtained for the thicker Ge layer is shown in Fig. 3. Here, we notice some structure on the Ge curves and a high value of the minimum yield compared to the silicon. Furthermore, the alignment of the curves is an indication of crystalline coherence between silicon and germanium. However, the narrowing along

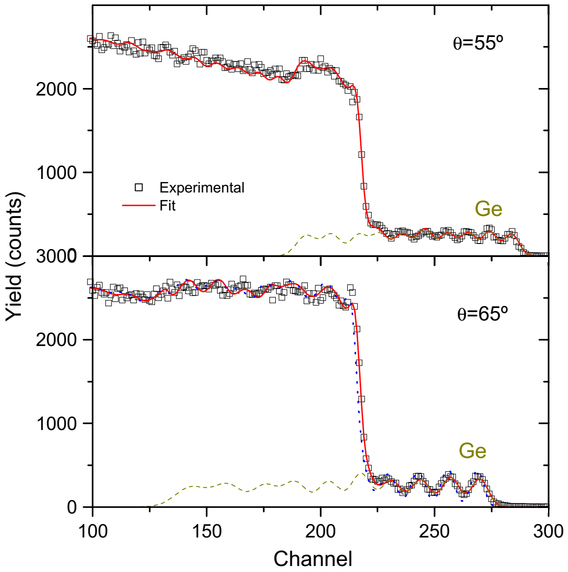

Fig. 1. RBS spectra collected at 55° and 65° for the sample 10 period Si/Ge multilayer. The solid lines show the fit considering interdiffusion. For 65° the fit for laterally homogeneous layers is shown as a dotted line.

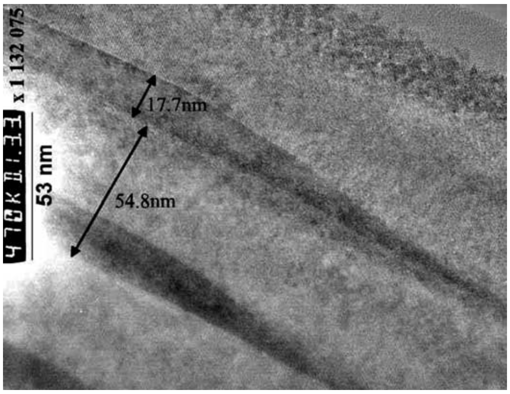

Fig. 2. TEM results for the 10 period Si/Ge multilayer where the presence of Ge quantum dots is observed.

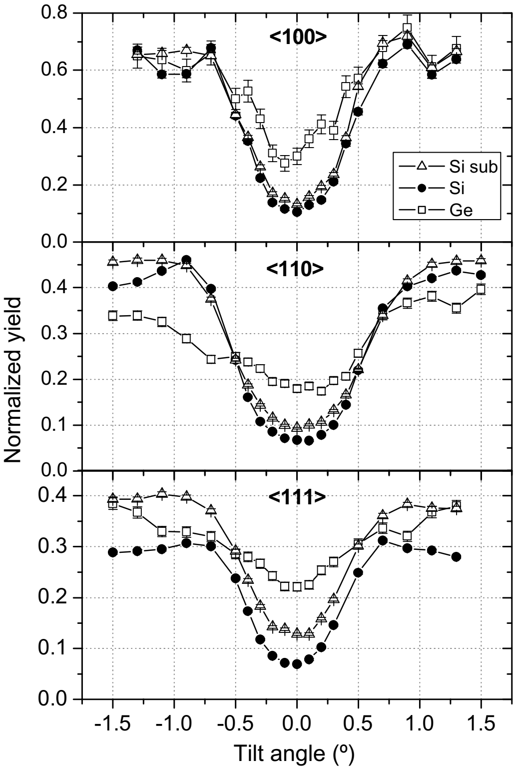

Fig. 3. Angular scans along the main axial directions for the 0.9 nm buried Ge layer. The broadening of the Ge curve for the ⟨1 1 0⟩ and the high value of the minimum yield suggest the formation of Ge precipitates.

the ⟨1 0 0⟩ and broadening along the ⟨1 1 0⟩ directions of the Ge curves compared to the silicon could indicate the presence of Ge precipitates. High resolution TEM are planned to check these assumptions necessary to support a model to simulate the results.

This study is a clear example of the capabilities of ion beam analysis where some of the other techniques show some limitations. In particular the Ge monolayers were out of range of X-ray diffraction studies and very difficult to measure by normal TEM.

3.2. FePt nanoparticles

The measured stoichiometry of the FePt nanoparticles obtained from the RBS data is 1:1 within the experimental error (5%). The RBS data collected for the C/FePt/C sample grown at 500 °C for three tilt angles are shown in Fig. 4. It is clear that the fit obtained assuming continuous C and FePt layers, does not reproduce the experimental data. The analysis of multilayers composed of equally spaced layers of nanoparticles embedded in the matrix is a complex problem. Recently, a method was proposed whereby, for some particular shapes of inclusions of known size, uniformly distributed over a single-layer, the corresponding spectrum can be calculated accurately [10]. Layer roughness can be included using the algorithm given in [11], where the roughness parameter is the standard deviation δX of the layer thickness in each point of the layer. The idea behind this approximation was the simulation of FePt thickness changing from point to point in the layer with a Gaussian (or Gamma) distribution. In this way, we could represent a layer containing nanoparticles, where the thickness of FePt changes from zero to the height of the largest particle, with a distribution given by the exact shape of the particles [12]. The fit obtained considering FePt particles with a flattened shape, around 0.8 nm in diameter and 3 nm in height distributed in quasi-continuous layers reproduces quite well the experimental data. Previously, we have confirmed the excellent agreement between the RBS results and HRTEM studies of identical samples [12]. The study of the samples grown at 20 and 800 °C showed that both

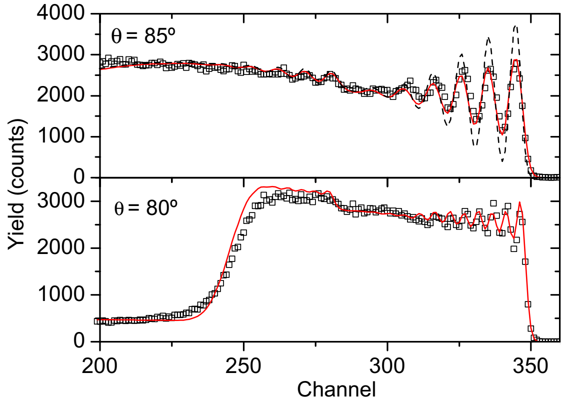

Fig. 4. RBS spectra collected at 80° and 85° for the sample grown at 500 °C. The fit considering FePt particles (solid lines) is shown. For 85°, a fit assuming pure layers with flat interfaces is also shown (dotted line).

the diameter and the height of the nanoparticles increase with deposition temperature. Since the amount of FePt deposited is the same in all samples the number of particles per layer must decrease. This result tells us that the size and number of the nanoparticles could be controlled playing with the growth temperature.

4. Conclusions

We studied Ge/Si and FePt/C multilayers grown at different temperatures. Using Rutherford backscattering at grazing angles of incidence, we determined the stoichiometry of the nanoparticles, the multilayer periodicity and the Ge strain. While the FePt layers consist of nanoparticles embedded in the C matrix the Ge/Si only indicate the presence of Ge quantum dots in the thicker layers.

Most importantly, we showed that the size of the nanoparticles increases with growth temperature, which can be used to control the magnetic properties of these systems. We compared the results with transmission electron microscopy results and showed the capabilities of ion beam analysis to get reliable information in some particular systems where most of the other techniques reveal several limitations.

Acknowledgements

This work was financed by Fundação para a Ciência e Tecnologia through the project POCTI/CTM/41918/2001 and in part by the INTAS Project No. 03-51-5015. We also thank D. Babonneau for the magnetic multilayers and the Ph.D. grant SFRH/BD/9013/2002 (NF).

References

[1] P. Schittenhelm, M. Gail, J. Brunner, J.F. Nützel, G. Abstreiter, Appl. Phys. Lett. 67 (1995) 1292.

[2] O.G. Schmidt, C. Large, E. Eberl, O. Kienzle, F. Ernst, Appl. Phys. Lett. 71 (1997) 2340.

[3] A.A. Shklyaev, M. Shibata, M. Ichikawa, Phys. Rev. B 62 (2000) 1540.

[4] M.L. Yan, H. Zeng, N. Powers, D.J. Sellmyer, J. Appl. Phys. 91 (2002) 8471.

[5] M. Miura, J.M. Hartmann, J. Zhang, B. Joyce, Y. Shiraki, Thin Solid Films 369 (2000) 104.

[6] A.V. Kolobov, A.A. Shklyaev, H. Oyanagi, P. Fons, S. Yamasaki, M. Ichikawa, Appl. Phys. Lett. 78 (2001) 2563.

[7] M. Derivaz, P. Noé, R. Dianoux, A. Barski, A. Coati, Y. Garreau, A. Alandi, Appl. Phys. Lett. 84 (2004) 3295.

[8] M. Watanabe, T. Masumoto, D.H. Ping, K. Hono, Appl. Phys. Lett. 76 (2000) 3971.

[9] N.P. Barradas, C. Jeynes, R. Webb, Appl. Phys. Lett. 71 (1997) 291.

[10] J.P. Stoquert, T. Szörényi, Phys. Rev. B 66 (2002) 144108.

[11] N.P. Barradas, E. Alves, S. Pereira, V.V. Shvartsman, A.L. Kholkin, E. Pereira, K.P. O'Donnell, C. Liu, C.J. Deatcher, I.M. Watson, M. Mayer, Nucl. Instr. and Meth. B 217 (2004) 479.

[12] N.P. Barradas, E. Alves, D. Babonneau, Nucl. Instr. and Meth. B 219–220 (2004) 919.